

Variability in finite-fault slip models of the 2011 Tohoku-Oki earthquake and implications for observationally constrained dynamic rupture simulations

Jeremy Wing Ching Wong^{1*}, Wenyuan Fan¹, Alice-Agnes Gabriel¹

¹ Institute of Geophysics and Planetary Physics, Scripps Institution of Oceanography, University of California San Diego

*Email: jeremywong@ucsd.edu

Introduction

Finite fault inversion often suffers from large uncertainties, which are poorly quantified. To understand the causes of the uncertainties and their implications, we collect 21 finite-fault slip models from the 2011 Tohoku-Oki Mw 9.1 earthquake and analyze their features in a unified framework with the same slab geometry. These finite-fault models are constrained using a variety of geophysical datasets and resolved using inversion methods. We develop a projection and upscaling scheme to consistently parameterize distinct finite-fault models. We then apply a suite of statistical analyses to extract the coherent part of the suit of models and address the variability among them.

Kinematic Models and Classifications

Dataset: 21 published finite-fault models of the 2011 Tohoku-Oki Mw 9.1 earthquake model (references in QR code)

Models are categorized based on the inversion datasets:

- 1 Static, geodetic
- 2 Regional, seismic (and geodetic)
- 3 Teleseismic, (and geodetic)
- 4 Static tsunami (and geodetic)
- 5 Joint tsunami, seismic, and geodetic

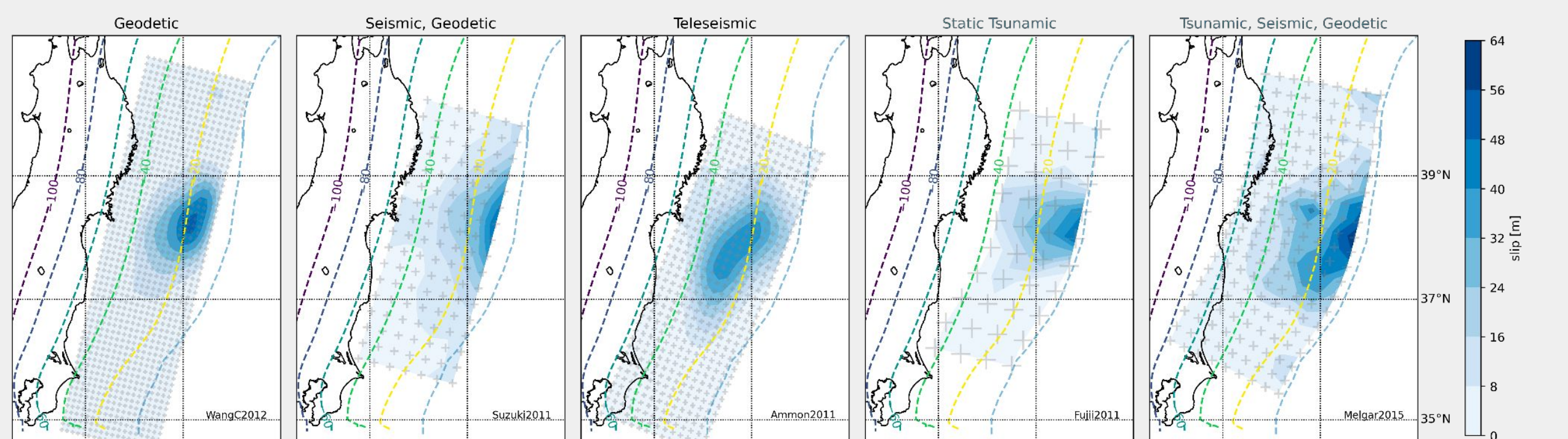


Fig 1 Five exemplary kinematic models of the Tohoku-Oki earthquake. Color-filled contours denote the slip distribution; gray markers denote the model parameterization. Color contours indicate slab geometry and trench location.

Projection and Upscaling the Kinematic Models

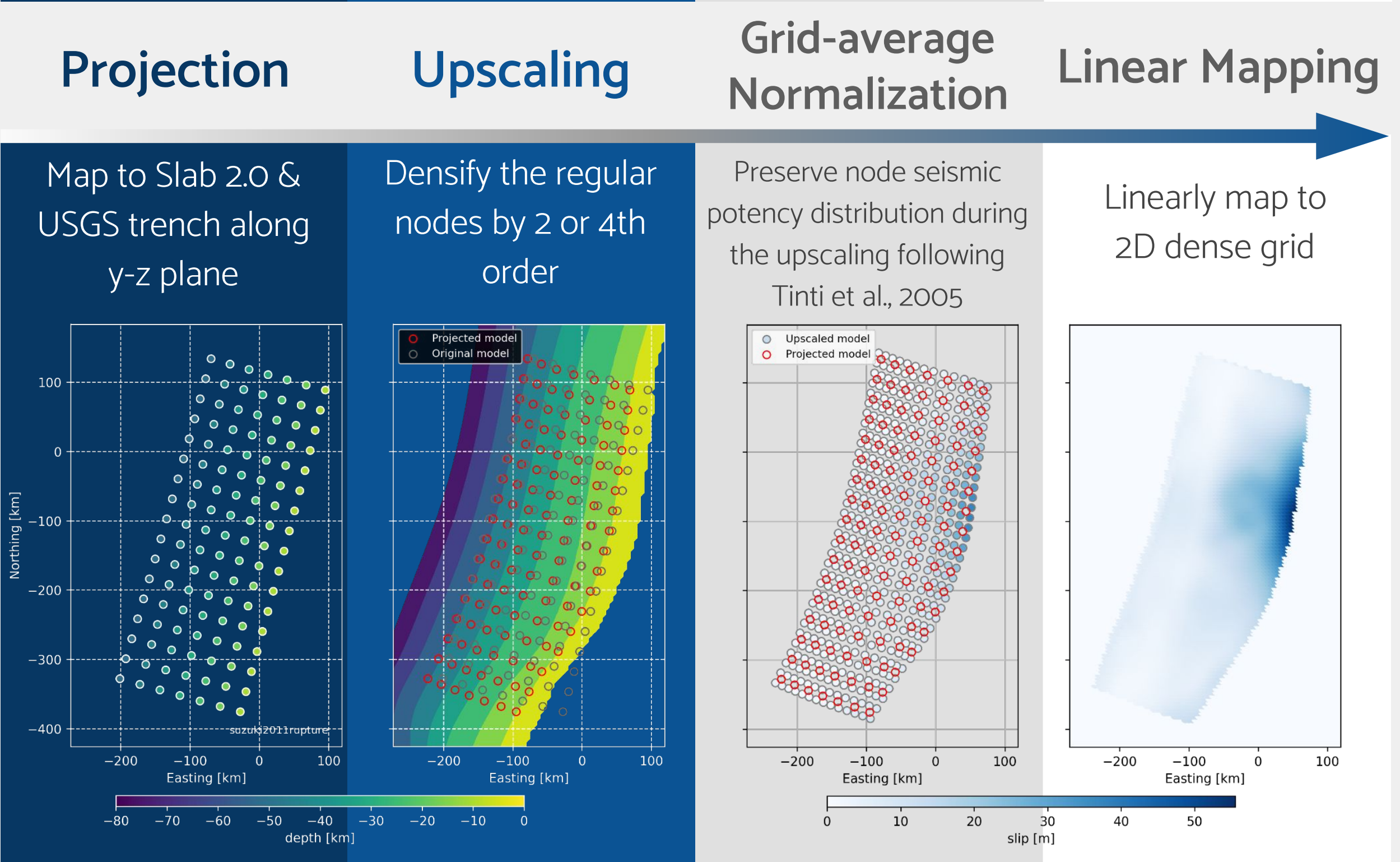
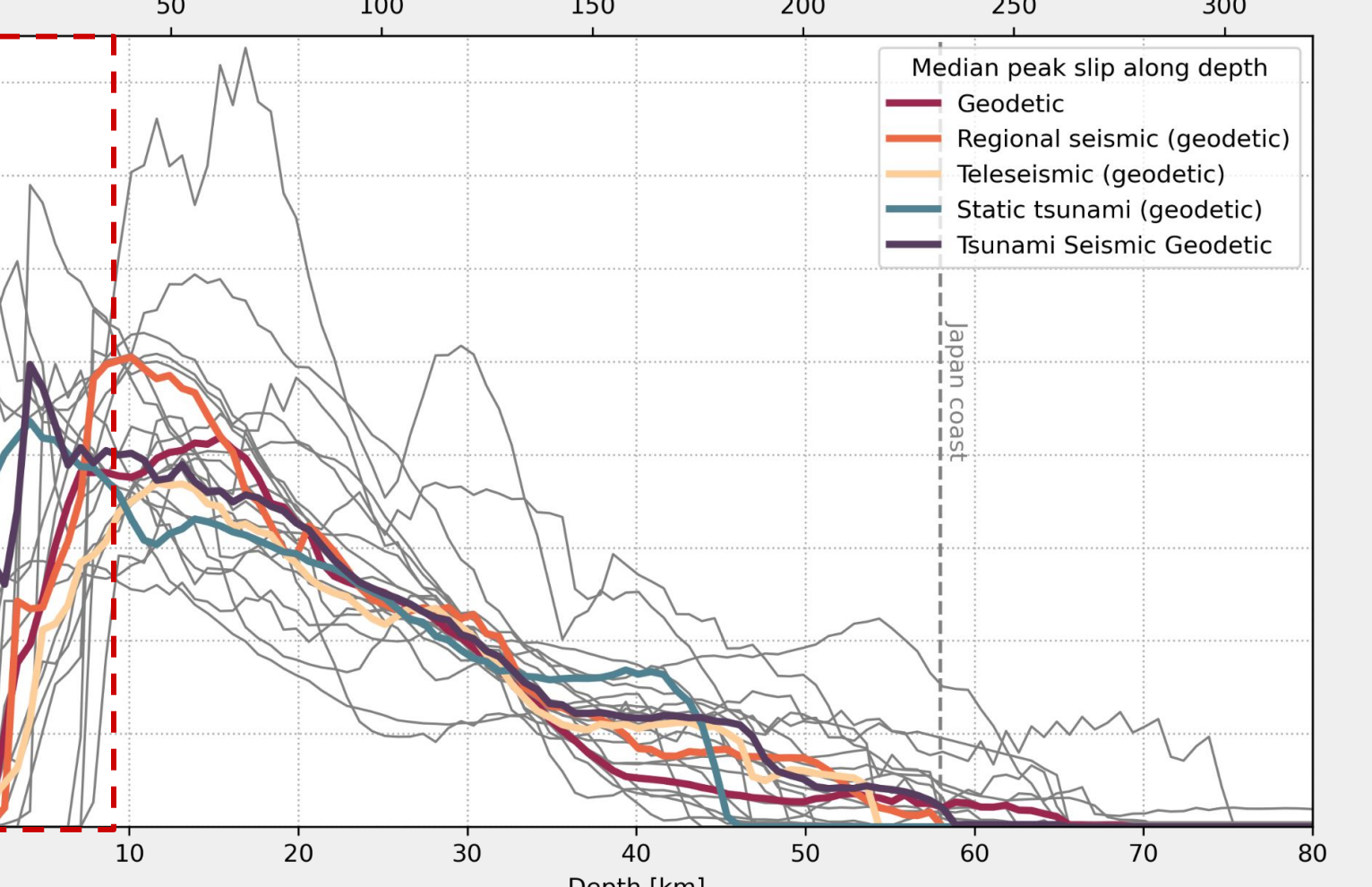


Fig 2 Projection and upscaling scheme for processing an example finite-fault slip model. Figures from left to right: 1 Original subfault parameterization, colored by depth; 2 Projecting a planar model to the curved slab geometry (Slab 2.0 and USGS trench (Hayes, G., 2018)), red circles denote the projected parameterization; 3 Upscaling the example model, colored by slip; 4 Linearly mapped dense regular grids, colored by slip.

Results: Along-Strike and Along-Depth Variation

We computed the peak slip distribution of each model along depth and strike directions. The median peak slip of each model category is shown in figure 3.

- ❖ The near-trench slip is prominent in models using tsunami data (blue and purple lines)
- ❖ The near-trench slip is absent in models without tsunami data (red, orange and yellow lines)
- ❖ Models using the regional seismic data suggest a greater peak slip at the 8 - 17 km depth
- ❖ The models are in agreement on slip at 20 km depth and deeper



- ❖ The peak-slip distribution are consistent along strike direction from -400 to 100 km.
- ❖ The northern extent of the slip is varying, extending from 200 km to 350 km north of hypocenter.

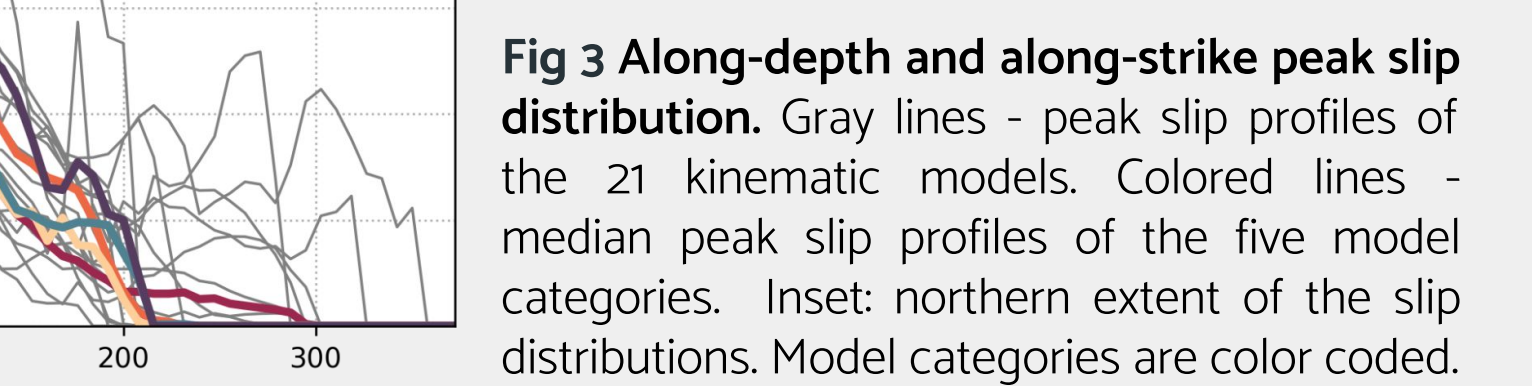


Fig 3 Along-depth and along-strike peak slip distribution. Gray lines - peak slip profiles of the 21 kinematic models. Colored lines - median peak slip profiles of the five model categories. Inset: northern extent of the slip distributions. Model categories are color coded.

Results: Spectral Analysis of the Slip Distribution

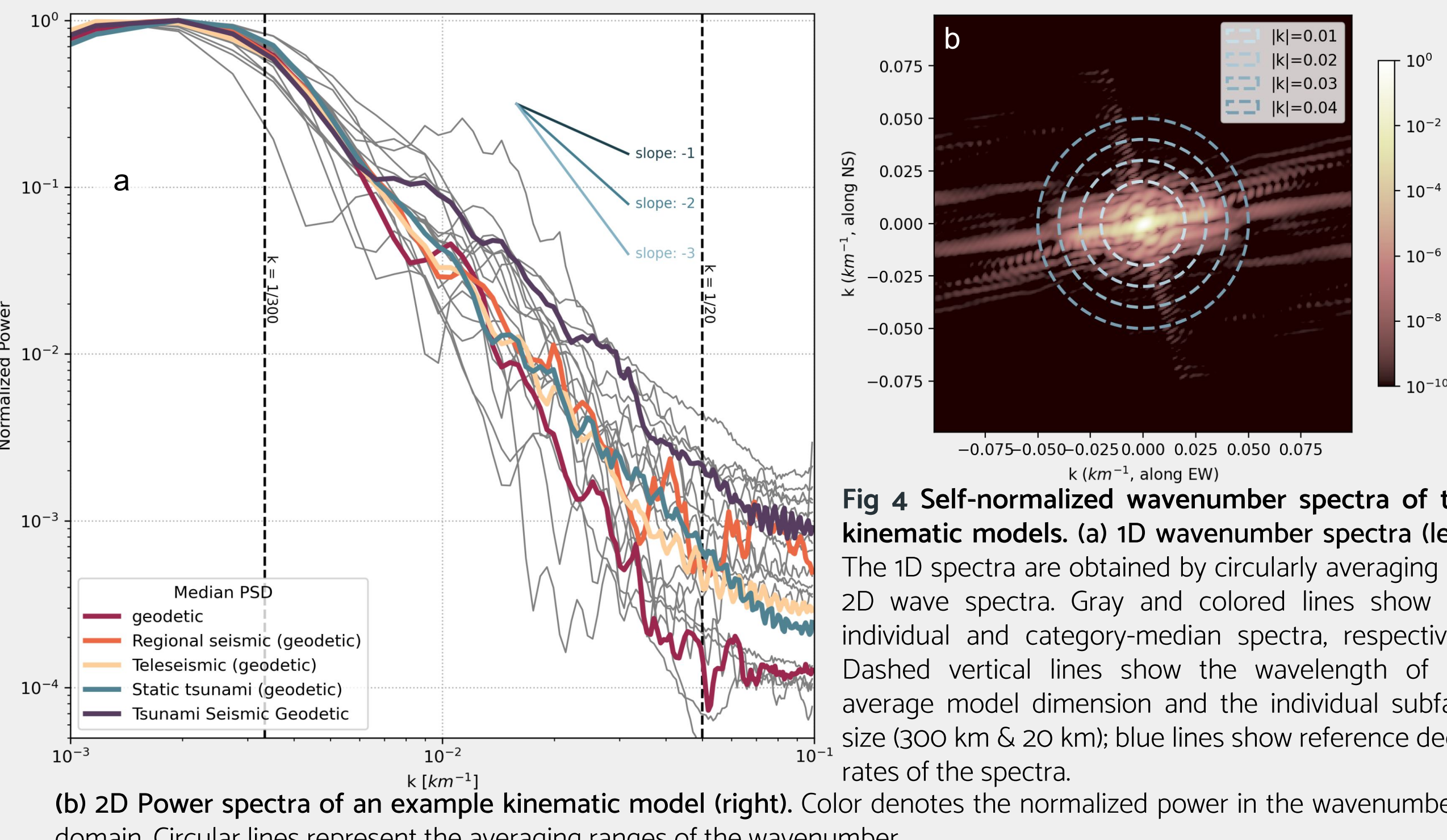


Fig 4 Self-normalized wavenumber spectra of the kinematic models. (a) 1D wavenumber spectra (left). The 1D spectra are obtained by circularly averaging the 2D wave spectra. Gray and colored lines show the individual and category-median spectra, respectively; Dashed vertical lines show the wavelength of the average model dimension and the individual subfault size (300 km & 20 km); blue lines show reference decay rates of the spectra. (b) 2D Power spectra of an example kinematic model (right). Color denotes the normalized power in the wavenumber domain. Circular lines represent the averaging ranges of the wavenumber.

We compute the 1D normalized power spectra of the kinematic models by averaging 2D power spectrum at each wavenumber radius, circularly averaging the spectrum as shown in figure 4b, following the method by Mai & Beroza 2002.

- ❖ Joint tsunami models have the lowest decay rate in their power spectra, indicating a higher degree of slip complexity in space
- ❖ Geodetic slip models have the highest decay rate compared to other slip models

Results: Correlation Analysis

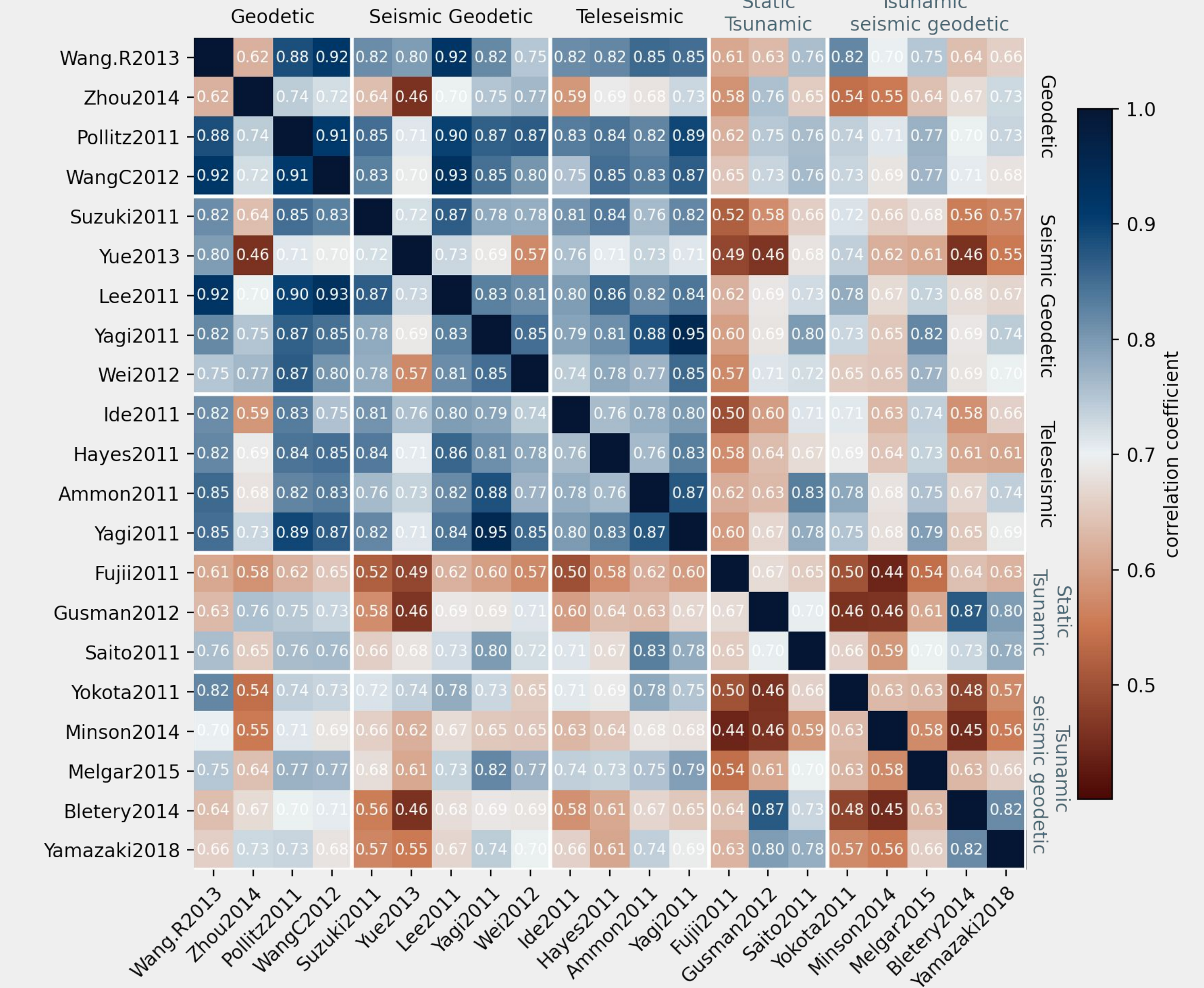


Fig 5 Correlation matrix of the kinematic models. Each entry shows the correlation coefficient between two models, with background color denoting the correlation coefficient. The correlation matrix is sorted by the model categories.

The correlation coefficient between each model is computed as the inner product between two normalized vectorized slip models.

- ❖ The average correlation is 0.71 with a standard deviation of 0.11.
- ❖ High correlation values (> 0.7) between models without using tsunami data (Geodetic, Seismic [\pm geodetic], Teleseismic [\pm geodetic] classes) with a median of 0.81.
- ❖ Low correlation (< 0.7) between models using tsunami data for inversion (static tsunami and joint tsunami seismic, geodetic classes) with a median of 0.63.
- ❖ Low correlation between models with and without tsunami data. The median correlation is 0.68.

Summary and Future Work

- ❖ Near trench slip shows strong variability among the models when analyzed across the curved slab geometry. The categorized model comparison underscore a systematic difference between model with and without the tsunami dataset.
- ❖ Along-strike slip distribution shows consistency among the models with notable variability of the northern extent of the slip distribution.
- ❖ Spectral analysis shows that tsunami data requires higher spatial degree of complexity in the associated slip models.
- ❖ Correlation analysis shows a higher similarity between models without using tsunami data than the models using tsunami data.
- ❖ Validation of the projection and upscaling scheme will be conducted including sea floor displacement and GEONET dataset comparison.
- ❖ Kinematic models will be used to compute initial stresses to drive the 3D dynamic rupture simulations (e.g. Tinti et al., EPSL 2021).

Selected Reference:

- [1] Tinti, E., Spudich, P., & Cocco, M. (2005). Earthquake fracture energy inferred from kinematic rupture models on extended faults. Journal of Geophysical Research: Solid Earth, 110(B12).
- [2] Mai, P. M., & Beroza, G. C. (2002). A spatial random field model to characterize complexity in earthquake slip. Journal of Geophysical Research: Solid Earth, 107(B11), ESE-10.
- [3] Tinti, E., Casarotti, E., Ulrich, T., Taufiqurrahman, T., Li, D., & Gabriel, A. A. (2021). Constraining families of dynamic models using geological, geodetic and strong ground motion data: The Mw 6.5, October 30th, 2016, Norcia earthquake, Italy. Earth and Planetary Science Letters, 576, 117237.

